# Radial Field Retrieval in Spherical Scanning for Current Reconstruction and NF–FF Transformation

Fernando Las-Heras and Tapan K. Sarkar, *Fellow, IEEE*

***Abstract*—In this paper, a near-field to far-field (NF–FF) transformation for the case of spherical scanning using equivalent magnetic currents (EMCs) and matrix methods is addressed. It is based on the decoupling of the field components and the iterative retrieval of the radial component of the electric field. The technique is applied for far-field calculation as well as for the estimation of the current distribution of the antenna under test (AUT) using spherical near-field facilities. Results from measured near-field data of several antennas are presented and compared to those of the analytical solution via a spherical wave mode expansion method.**

***Index Terms*—Equivalent sources, near-field (NF) far-field (FF) transformation.**

## I. Introduction

NEAR-FIELD scanning over canonical surfaces—planar, cylindrical, and spherical—is often used to obtain the far-field pattern characteristics of an antenna under test (AUT) via near-field to far-field (NF–FF) transformation algorithms. Spherical scanning is most versatile in the sense that it makes it possible to obtain the radiation pattern over the entire angular span of any arbitrary antenna. Spherical NF–FF transformation techniques based on a modal expansion in spherical waves has been widely used [1], [2]. In these techniques, the convergence of the series representation makes it necessary to have a knowledge of the near field over an angular interval sufficiently greater (depending on the maximum AUT dimension and acquisition distance) than the desired far-field angular interval. Diagnosis tasks in those techniques, can be done through the Fourier transform to obtain the aperture field from the far field.

Finally, NF–FF transformation [3] and diagnosis [4] can be accomplished using arbitrary scanning surfaces with a matrix method formulation based on the reconstruction of some equivalent current distribution over that arbitrary surface. One characteristic of the matrix techniques is that it gives the best far-field solution (in the least squares sense) for a given near-field data set. In this way, it has been experimentally observed that near-field scanning is only required in the desired far-field angular interval. The intermediate step of source reconstruction inherent in a matrix method formulation yields the possibility of performing diagnosis tasks in some type of antennas, such as planar arrays and aperture antennas, since the method gives the best solution of the equivalent sources (field at the aperture) for a given near-field data set. However, a large system of equations appears when directly applying numerical matrix methods to the resultant integral equations relating source components and electric field components.

In fact, in a general equivalent problem for spherical near-field scanning, two components (tangential to the surface enclosing the AUT) of both the equivalent magnetic and equivalent electric currents must be used. When reconstructing over an infinite plane, only one type of equivalent currents can be used, but still two components of this equivalent currents are needed. So, finally, two coupled integral equations arise when relating electric field components (angular components over the spherical scanning surface) and the equivalent source components along an infinite plane (the antenna plane). When solving numerically the integral equations one needs to solve a large system of equations.

In this paper, after establishing the equivalent problem with only an equivalent magnetic current (EMC) distribution, an alternate formulation is presented. The formulation is based on the decoupling of the two integral equations under an assumption of a zero value of the radial component of the electric field. Then, each integral equation can be solved independently for each component of the EMC. The numerical solution of each integral equation is performed by minimizing a least squares error functional. This approach works well when measurements are performed in the Fresnel region [4]. For a more general acquisition distance and in order to overcome the limitations resulting from neglecting the radial electric field, an iterative algorithm that retrieves the radial component of the electric field is proposed.

In order to compare this technique with the modal expansion technique, a numerical code utilizing the NF-FF transformation based on a wave mode expansion [2] has been used to calculate the radiation patterns from synthesized and measured near-field data. Synthesized data from radiating configurations, where the radial component of the electric field cannot be neglected, have been used to assess the accuracy of this method. Results using both the radial field retrieval technique and the modal expansion technique have been presented for most of the examples.

Special attention has been paid to experimental validation. The measured near-field data from a reflector antenna has been used to calculate the far-field pattern and to reconstruct the field at the antenna aperture. Also, the analytical solution for the

Manuscript received October 30, 2000; revised June 6, 2001. This work was supported in part by Spanish DGES of the Ministerio de Educación y Cultura.

F. Las-Heras is with the Universidad Politecnica de Madrid, ETSI Telecomunicacion, Ciudad Universitaria, 28040-Madrid, Spain (e-mail: fernando@gr.ssr.upm.es).

T. K. Sarkar is with Department Electrical Engineering and Computer Science, Syracuse University, Syracuse, NY 13244 USA (e-mail: tksarkar@mailbox.syr.edu).

Publisher Item Identifier S 0018-926X(02)05747-2.

far-field pattern with a wave expansion method has also been calculated for comparison purposes. Other measured data have been used to illustrate the applicability of the proposed radial field retrieval technique.

## II. Equivalent Current Reconstruction From Spherical Data

To reach the final matrix formulation, an equivalent problem is established with an EMC distribution over an infinite plan that coincides with the antenna plane (aperture plane, layer of impressed radiating elements in the case of two-dimensional (2-D) arrays, or a virtual plane "enclosing" the antenna). For numerical purposes, the domain of this EMC distribution is truncated at some distance from the antenna where the tangential electric field can be neglected. Then, for the external equivalent problem, a relation between the field radiated by the original AUT and the EMC density distributed over the plane $S'$ can be written as the vector integral equation

$$\vec{E}(\vec{r}) = \Im\left(\vec{M}_{se}(x', y')\right) \tag{1}$$

where $\Im$ is an integral operator that includes the Green function in an unbounded medium. Considering the particular case of spherical scanning, two scalar integral equations appear in such a way that each angular component of the electric field depends on both the Cartesian components of the EMC density. Therefore

$$\begin{aligned} E_\theta(R_o, \theta, \varphi) &= \Im_1(M_x, M_y)\\ E_\varphi(R_o, \theta, \varphi) &= \Im_2(M_x, M_y). \end{aligned} \tag{2}$$

Under this standard representation, a great number of unknowns representing the EMC distribution are typically involved in the numerical solution of this system of integral equations. However, two independent integral equations can be obtained if we neglect the radial component of the measured near field. Under this assumption, the Cartesian components of the electric field can be obtained from the acquired angular components of the electric field with the following approximation:

$$\begin{bmatrix} E_x \\ E_y \end{bmatrix} = \begin{bmatrix} \cos\theta\cos\varphi & -\sin\varphi \\ \cos\theta\sin\varphi & \cos\varphi \end{bmatrix} \begin{bmatrix} E_\vartheta \\ E_\varphi \end{bmatrix}. \tag{3}$$

Now, an integral equation relating the Cartesian EMC components and Cartesian field components can be used. If the observation point is represented by the spherical coordinates $(R_o, \theta, \varphi)$ and the source points are represented by the Cartesian components $(x', y', z'_0)$, then the field due to an EMC distribution over the $S'$ plane can be written as [8]

$$\begin{aligned} &E_x(R_o, \theta, \varphi)\\ &\quad = -\int_{S'} M_y(x', y') \cdot G(\lambda, R_o, \theta, \varphi, x', y', z'_0)\, ds' \end{aligned} \tag{4}$$

TABLE I
Nominal Values of 2-D EMC Distribution

| | |
|---|---|
| Frequency | 1,5GHz |
| Dimensions, LX x LY | 1m x 1m (5λ x 5λ) |
| My (amplitude) | $1/(1+x^2+y^2)$ |
| My (phase) | $45(\sqrt{x^2+y^2}/LX)$ , deg |
| Mx (amplitude) | $0.01+x^2+y^2$ |
| Mx (phase) | 0 , deg |
| Acquisition distance | 0,8m (4λ) |

$$\begin{aligned} &E_y(R_o, \theta, \varphi)\\ &\quad = \int_{S'} M_x(x', y') \cdot G(\lambda, R_o, \theta, \varphi, x', y', z'_0)\, ds' \end{aligned} \tag{5}$$

$$\begin{aligned} &G(\lambda, R_o, \theta, \varphi, x', y')\\ &\quad = (R_o\cos\theta - z'_0)\left(\frac{1+j\beta R}{4\pi R^3}\right)e^{-j\beta R} \end{aligned} \tag{6}$$

where $\lambda$ is wavelength $\beta$ is the wavenumber, and $R$ is the distance between each source points and the observation point. The advantage of this representation is that two decoupled integral equations are obtained, each relating one Cartesian component of the electric field to one Cartesian component of the EMC distribution. Only half the number of unknowns of the conventional matrix representation derived from (2) is involved in the solution of each of the integral equations.

Each of the integral equations (4) and (5), relating the field components to the EMC components, are solved numerically. This is done by expanding each EMC in terms of a subdomain-type basis function and then determining their amplitudes through the minimization of a cost function.

Let us represent the scalar measured data corresponding to one of the electric field components by the vector $Y$ which is due to an EMC $M_e$, by the vector $E$; so that $E = GM_e$. Here $M_e$ is the vector corresponding to a discretized representation of the corresponding EMC component over the surface $S'$. Then a positive semidefinite cost function can be defined

$$\chi = (GM_e - Y)^T (GM_e - Y)^*. \tag{7}$$

From (7), a quadratic form in $M_e$ can be easily obtained

$$\chi = M_e^T H M_e^* + \left(M_e^T B + B^{T*} M_e^*\right) + C \tag{8}$$

where $H = G^T G^*$ is related to the Hessian matrix, $B = -G^T Y^*$, $C = Y^T Y^*$ and $M_e^T$, $M_e^*$ are the transpose and conjugate, respectively, of the vector representing the EMC distribution. Then the optimization procedure to obtain $M_e$ reduces to finding the minimum of the quadratic form. By taking the first derivative and setting it to zero, results in

$$M_{e,\mathrm{opt}} = H^{-1} B^*. \tag{9}$$

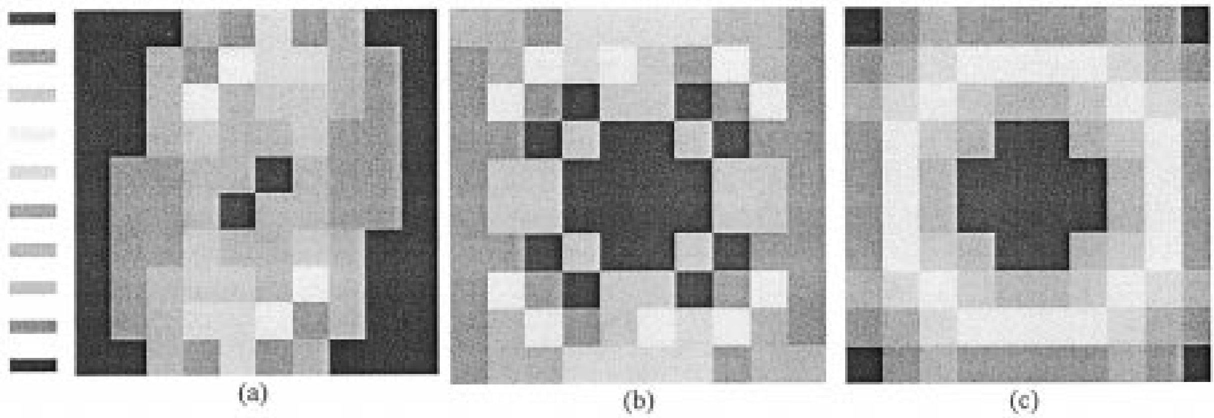

Fig. 1. Amplitude (in decibels) of the EMC $M_y$. (a) Reconstructed with one iteration. (b) Reconstructed with 20 iterations. (c) Nominal. Color scale: (−3, 0).

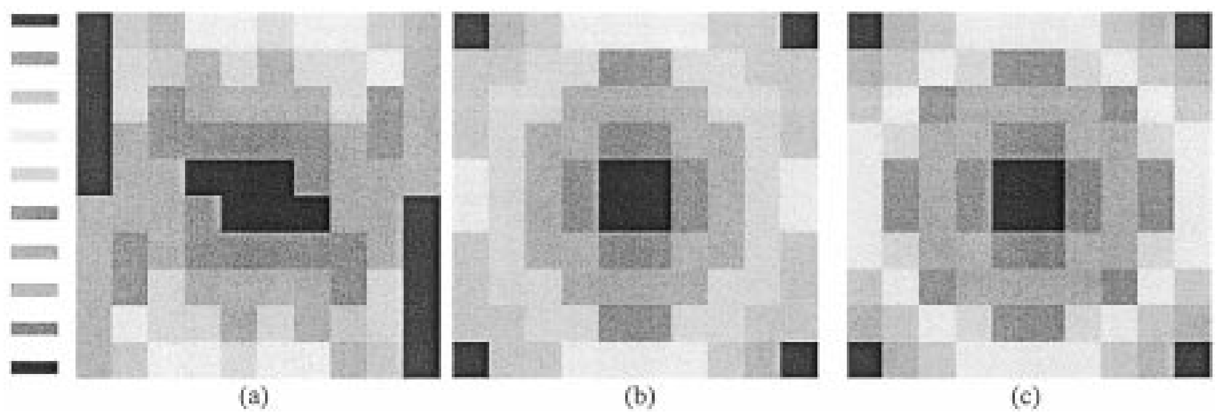

Fig. 2. Phase (in degrees) of the EMC $M_y$. (a) Reconstructed with one iteration. (b) Reconstructed with 20 iterations. (c) Nominal. Color scale: (5, 60).

## III. Radial Electric Field Retrieval Algorithm

The approximation used in (3) can provide good results in certain cases when measuring in the Fresnel region of a test antenna in a near-field spherical scanning range. However, the above formulation is not general and is not accurate under general conditions. If due to the electric size of the antenna and the scanning distance, it can happen that the values of the angular components of the electric field are no longer greater than the radial component, hence, the radial component of the electric field cannot be neglected and one cannot use directly the formulation established in (3)–(6).

In order to evaluate the radial component of the electric field when transforming to the Cartesian components from its angular components, an iterative algorithm for the radial field retrieval is proposed. As a starting point, the value of the radial component of the electric field is set to zero and an initial EMC reconstruction step is performed according to the formulation previously presented. With this first estimate of the EMC distribution, the electric field over the hemispherical scanning surface is calculated, replacing the zero values of the radial component by the calculated ones at each scanning point. Now the Cartesian components of the measured field are calculated using both the angular and radial field components. A new EMC is then computed. The iterative procedure continues until the predefined accuracy of the solution is achieved. The steps of the algorithm are summarized as follows.

1) Start with an initial guess for the EMC components $M_{e,y}^0$, $M_{e,x}^0$.
2) Set to zero initially the value of the radial component of the electric field. The Cartesian components of the electric field $E_x^0$, $E_y^0$ are obtained from the scanned angular components $E_\theta$, $E_\varphi$ using the approximation (3).
3) Reconstruct each component of EMC by solving the integral equations (4) and (5) for $M_{e,y}^{k\,iter}$, $M_{e,x}^{k\,iter}$, respectively.
4) Calculate the radial component of the electric field $E_r^{k\,iter}$, from the magnetic current components $M_{e,y}^{k\,iter}$, $M_{e,x}^{k\,iter}$.
5) Calculate of the Cartesian components of the electric field $E_x^{k\,iter}$, $E_y^{k\,iter}$, from the scanned angular components $E_\theta$, $E_\varphi$, and the estimated radial component $E_r^{k\,iter}$.
6) Go to 3) for the next iteration.

## IV. Results

### A. Synthesized Results

*2-D Magnetic Current Distribution:* First, synthesize near-field data from a known EMC distribution. This is then used to verify the proposed radial reconstruction algorithm. An ac-

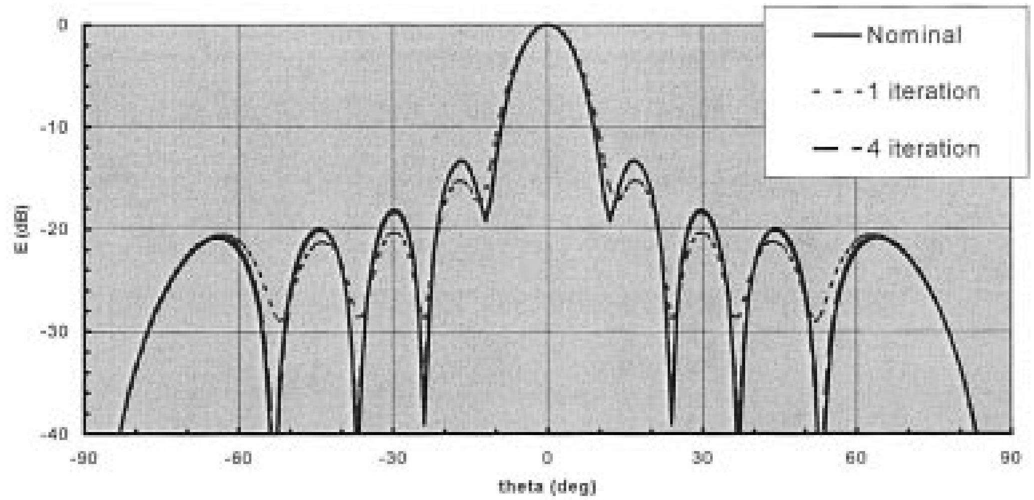


Fig. 3. 2-D EMC distribution. Far-field pattern ($\varphi = 0°$) from nominal and reconstructed sources.

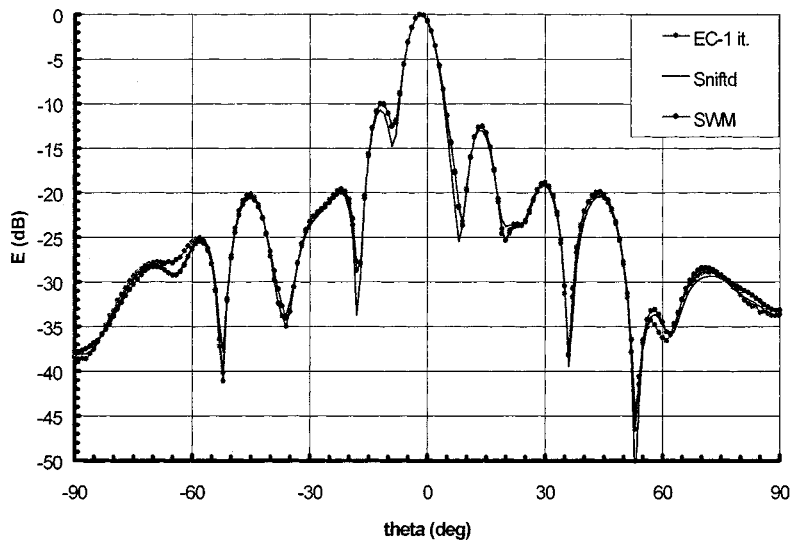


Fig. 4. Linear patch array. Far-field pattern ($\varphi = 0°$). Copolar.

quisition distance, close enough to the radiating structure, has been selected so that the radial component of the electric field cannot be neglected. The nominal EMC distribution, from the near-field data have been synthesized, as well as other parameters of the simulation are described in Table I. Scanning increments of $\Delta\theta = 1°$ and $\Delta\varphi = 1°$ have been considered for synthesizing the near-field data; and a discretization of the source domain using $10 \times 10$ source cells has been considered for the near-field synthesis as well as for the source reconstruction.

In Figs. 1 and 2, the reconstructed EMC distribution (amplitude and phase of the $M_y$ component) for various iterations of the radial field retrieval algorithm are compared to the nominal EMC distribution. In Fig. 3, a comparison between the far-field pattern due to the nominal EMC distribution and the far-field pattern calculated from the reconstructed EMC distribution for several iterations of the radial field retrieval algorithm is presented.

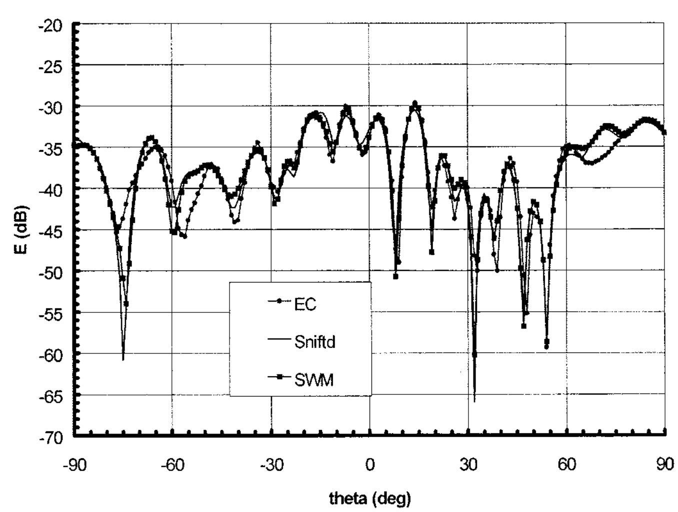


Fig. 5. Linear patch array. Far-field pattern ($\varphi = 0°$). Cross-polar.

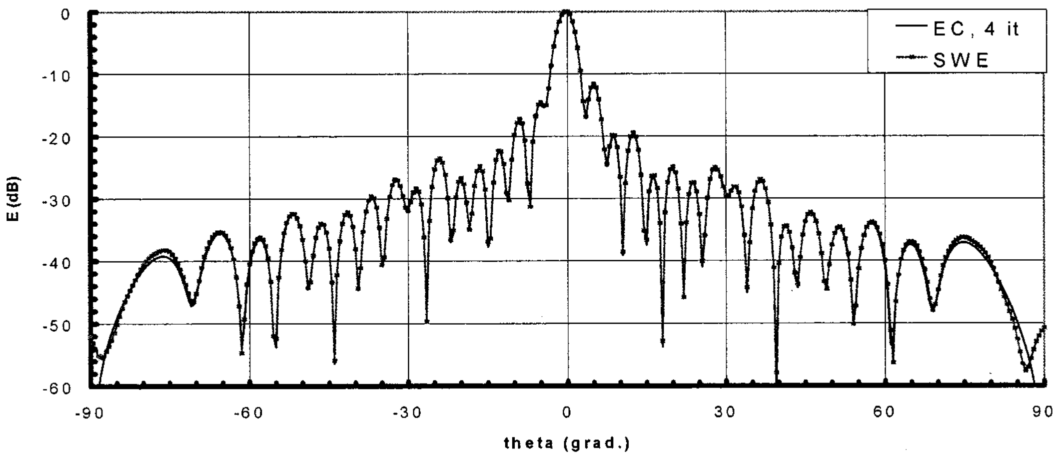


Fig. 6. 32 × 32 patch array. Far-field pattern ($\varphi = 0°$). Copolar.

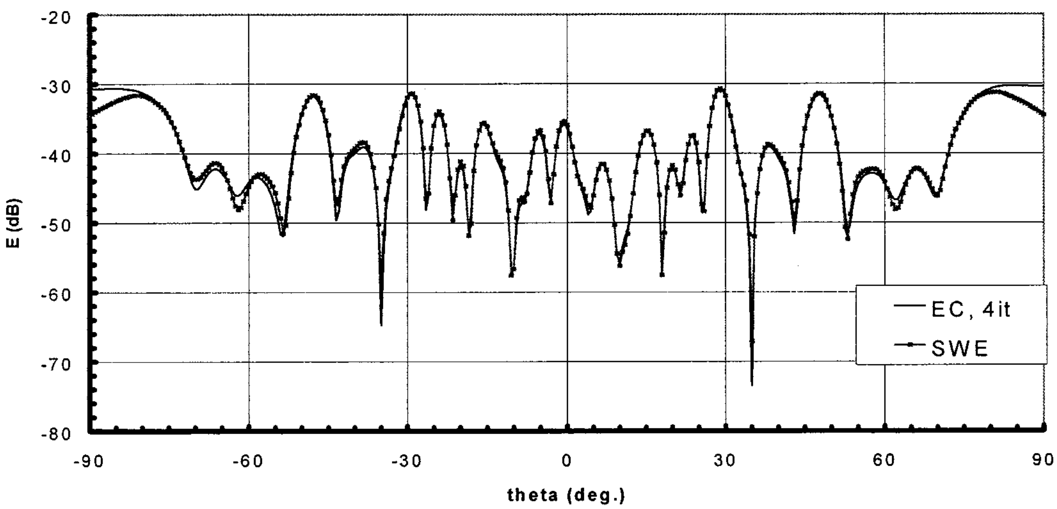


Fig. 7. 32 × 32 patch array. Far-field pattern ($\varphi = 0°$). Cross-polar.

### B. Measurement Results

*Linear Patch Array:* A commercial base-station antenna for mobile communications of 1.5-m length was measured at the near-field spherical facility of Grupo de Radiacion-Universidad Politecnica de Madrid, at a frequency of 1.8 GHz, with a scanning radius of 3.3 m and scanning increments of $\Delta\theta = 1°$ and $\Delta\varphi = 1°$. The calculated copolar and cross-polar components of the far field in the $E$-plane (polarization along the array direction) using the proposed numerical algorithm based on the equivalent currents as well as using the spherical wave expansion of [2] and the SNIFTD software [7] are shown in Figs. 4 and 5. In this case, no iterative process for the calculation of the radial field is needed (at iteration 1, zero value of the radial component is considered) to obtain results using the equivalent current algorithm. Near-field data in the front hemisphere have been used in the EMC algorithm while complete spherical near-field data are considered for the spherical wave expansion results. Under these premises, the calculation of the far field in the front region (32 851 points) with the equivalent current-radial field retrieval algorithm is 17 times faster than with the spherical wave expansion method.[2].

*32 × 32 Patch Array:* The near-field data of a square planar array of 32 × 32 patches, at 3.3 GHz, measured over a spherical surface of radius 1.23 m was used to validate the proposed algorithms. This data set which is referred to in the iterative radial field retrieval algorithm, the field at the antenna plane (EMC distribution), and the far-field pattern in the main planes were calculated. The results of the copolar far field in the main planes are compared to the results of the analytical spherical wave expansion technique in Figs. 6 and 8. The results of the EMC technique have been calculated with four iterations of the radial field retrieval algorithm. Results with both techniques are undistinguishable except close to grazing angles, where discrepancies are due to the truncation of the equivalent current domain that imposes a zero value of the tangential electric field outside this domain in the EMC technique. The degree of agreement in the cross-polar results with both the techniques can be observed in Figs. 7 and 9. The reconstructed electric field at the plane of the antenna, in both amplitude and phase, are shown in Fig. 10, where a 1.6-m × 1.6-m domain and 64 × 64 cell elements were used to reconstruct the EMC. In Fig. 10, the outlines of the radiating structure are visible.

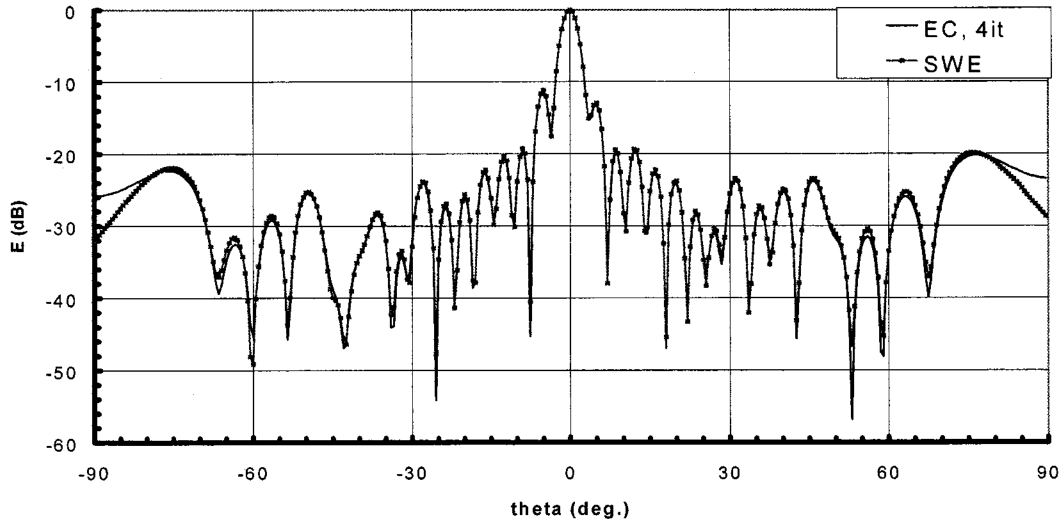


Fig. 8. 32 × 32 patch array. Far-field pattern ($\varphi = 90^\circ$). Copolar.

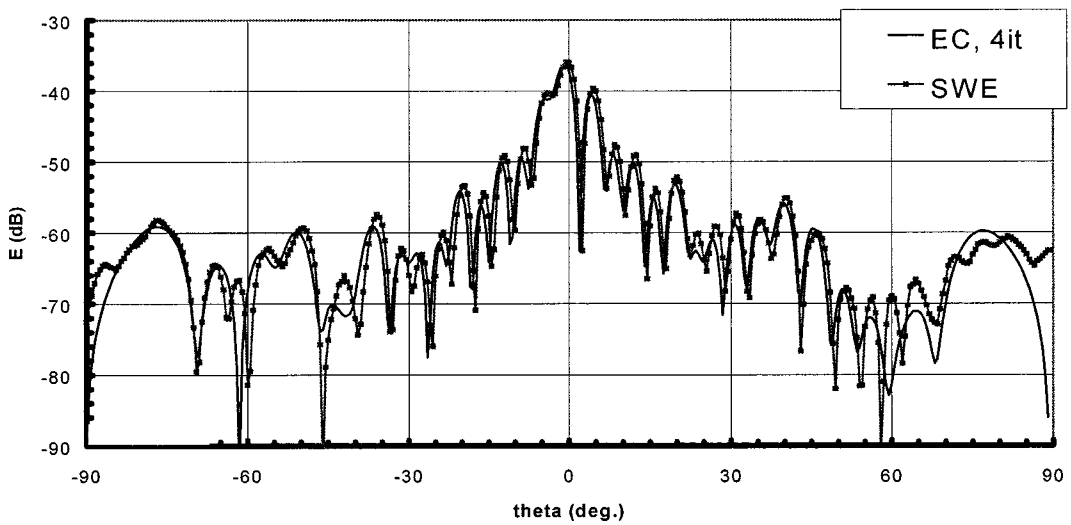


Fig. 9. 32 × 32 patch array. Far-field pattern ($\varphi = 90^\circ$). Cross-polar.

For a complete far-field pattern in the front of the antenna with 1° increment for both the angular coordinates, the equivalent current–radial field retrieval algorithm results are achieved in a CPU time five times faster than the CPU time used with the spherical wave mode expansion algorithm with 134 modes.

*90-cm Reflector Antenna:* An aperture antenna has also been used for experimental verification. For that purpose, the near field data of a 90-cm reflector antenna was measured on the spherical near-field range of the Laboratorio Ensayos (El Casar de Talamanca, Madrid). The radial distance of the spherical scanning was 126 cm and the frequency of operation was 10.7 GHz. For this configuration, the AUT produces an electric field with some nonnegligible radial component. Only scanned near-field data in the range $\theta \in [0^\circ, 40^\circ]$, $\varphi \in [0^\circ, 360^\circ]$, with angular increments $\Delta\theta = 0.5^\circ$ and $\Delta\varphi = 0.75^\circ$, were used as input for the source reconstruction–radial field retrieval algorithm. The far-field pattern results are shown in Figs. 11–14. Even for this close acquisition distance, it can be seen that reliable far-field results can be obtained for the copolar $\varphi = 0^\circ$-plane without performing radial component retrieval (iteration 1). However, in some directions, the zero radial field assumption is not accurate enough. This is the case for the cross-polar far field in the $\varphi = 90^\circ$-plane, whose results are shown in Fig. 14. In that plane, if the radial field component is neglected, the proposed EMC reconstruction gives a far-field result that differs from the one obtained with spherical wave expansion at levels around −30 dB near the broadside $\theta = 0^\circ$ direction. However, after a complete iteration of the radial field retrieval algorithm, the calculated results agree with those of the wave expansion method. Segmentation of the source domain using 80 × 80 cells was performed for the EMC reconstruction purpose. The intermediate results of the amplitude of the EMC distribution (components of the tangential electric field) over a domain of 1 m × 1.2 m in the aperture plane are shown in Fig. 15; the circular geometry and the feeding blockage can be seen in this figure.

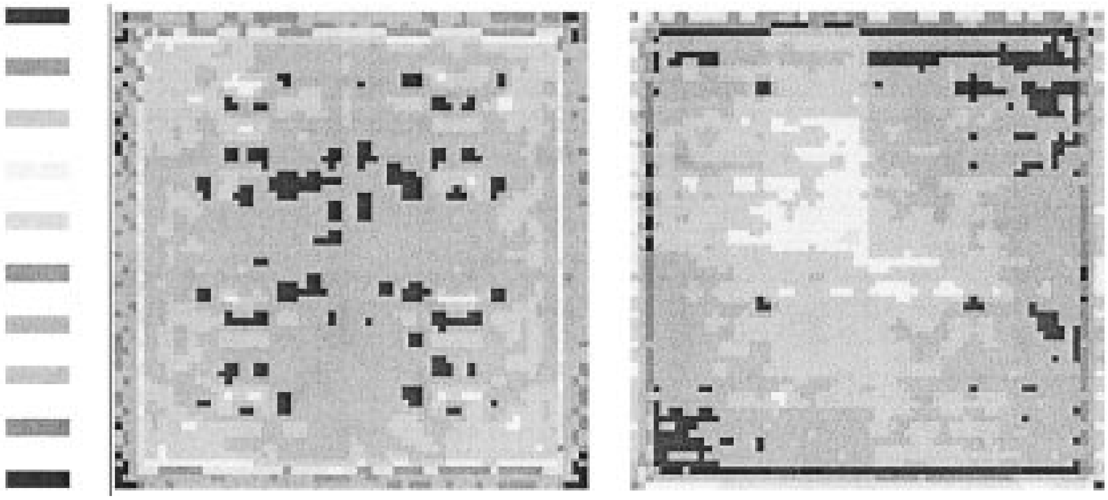

Fig. 10. 32 × 32 patch array. Amplitude (−30 dB/0 dB) and phase (−180°/180°) of the electric field at the antenna plane.

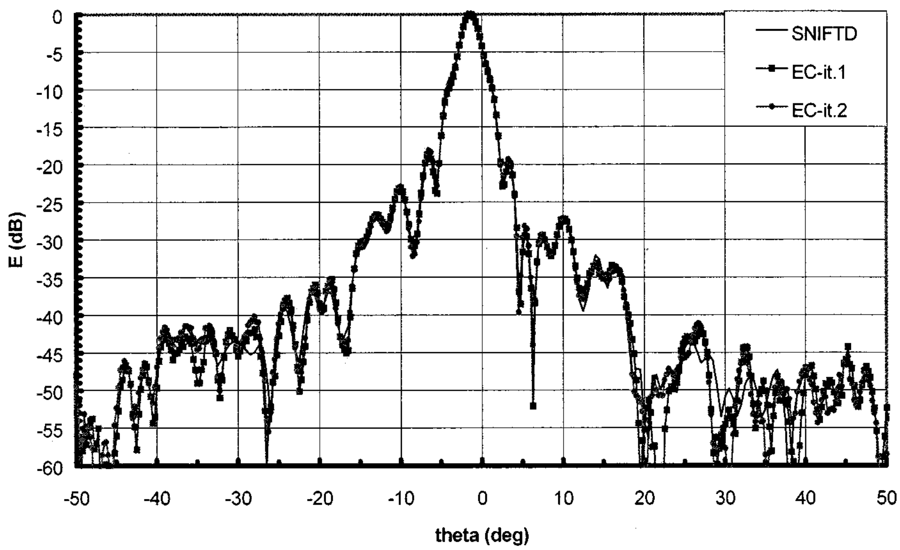


Fig. 11. Reflector—90 cm. Far-field pattern ($\varphi = 0°$). Copolar.

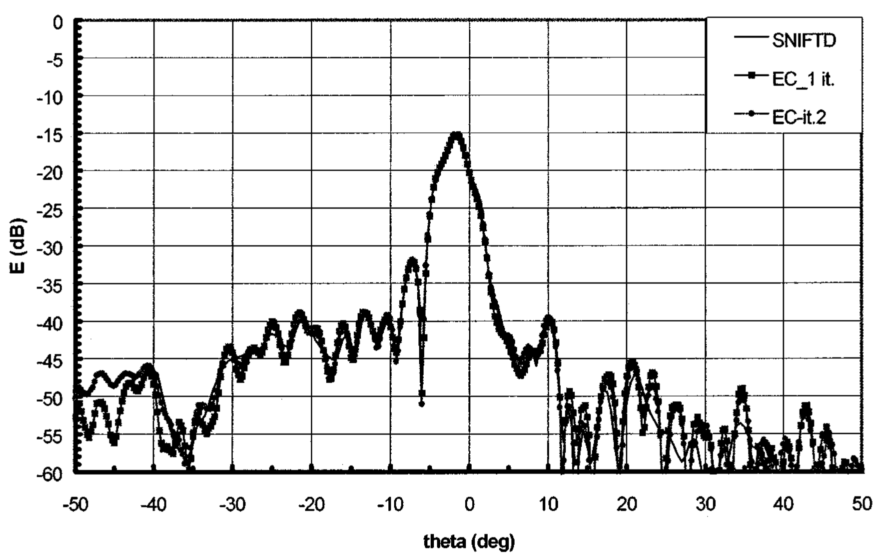


Fig. 12. Reflector—90 cm. Far-field pattern ($\varphi = 0°$). Cross-polar.

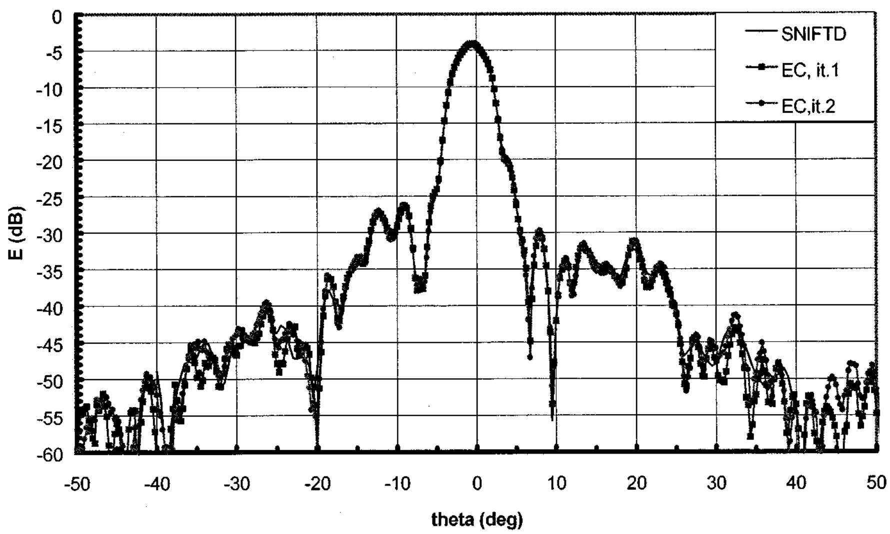


Fig. 13. Reflector—90 cm. Far-field pattern ($\varphi = 90°$). Copolar.

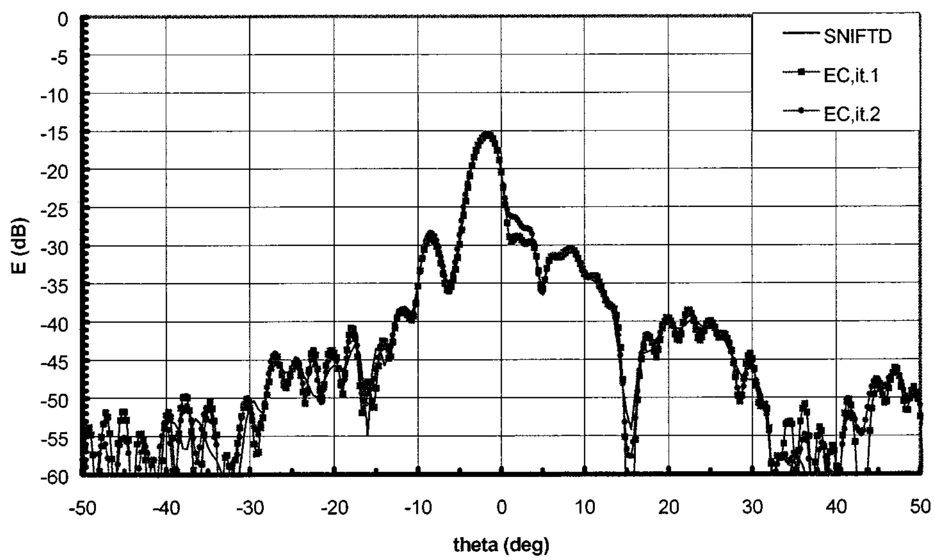


Fig. 14. Reflector—90 cm. Far-field pattern ($\varphi = 90°$). Cross-polar.

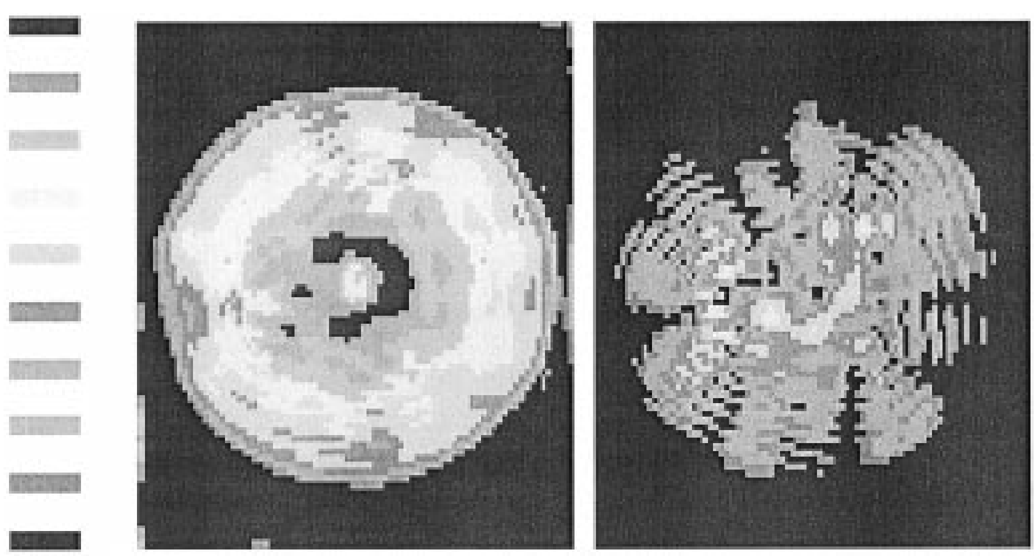

Fig. 15. Reflector—90 cm. Electric field components at the aperture (100 cm $\times$ 120 cm).

## V. Conclusion

An equivalent source reconstruction and NF–FF transformation method has been presented for the case of spherical scanning. The method makes use of a radial component retrieval algorithm in an iterative fashion. This algorithm is based on the decoupling of the integral equations appearing in the source reconstruction algorithm, reducing to half the number of unknowns that must be handled in the matrix solution and increasing the computational efficiency over traditional NF–FF matrix methods for the spherical scanning case. Just a few iterations are typically required for accurate NF–FF transformation while diagnosis can require more refinement. A comparison with the technique based on the spherical wave-mode expansion has been performed in terms of far-field results. The results of this comparison together with the computational efficiency and the possibility of performing direct diagnosis tasks, make the presented technique an interesting alternative in the area of near-field antenna measurements.

## Acknowledgment

The authors wish to thank the Laboratorio de Ensayos of El Casar de Talamanca, and Pr. J. L. Besada and P. Caballero for supplying the experimental data.

## References

[1] J. E. Hansen *et al.*, "Spherical near-field antenna measurements," in *IEE Electromagnetic Waves*, ser. 26. London, U.K.: Peter Peregrinus, 1988.

[2] T. K. Sarkar, P. Petre, A. Taaghol, and R. F. Harrington, "An alternative spherical near field to far field transformation," *Progr. Electromagn. Res.*, vol. PIER 16, pp. 269–284, 1997.

[3] P. Petre and T. K. Sarkar, "Planar near-field to far field transformation using an equivalent magnetic current approach," *Trans. Antennas Propagat.*, vol. 40, pp. 1348–1356, Nov. 1992.

[4] F. Las-Heras, B. Galocha, J. L. Besada, and P. Caballero, "Diagnosis of aperture antennas from measured near field data using ESLEST software," in *Proc. Antenna Measurement Techniques Association (AMTA), 20th Annu. Meeting & Symp.*, 1998, pp. 192–196.

[5] F. Las-Heras, "Near field to far field transformation using reconstruction of equivalent sources: Spherical acquisition," in *1999 USNC/URSI Dig.*, 1999, p. 60.

[6] ——, "Radial field retrieval for current reconstruction from spherical acquisition," *Electron. Lett.*, vol. 36, no. 10, pp. 867–869, May 2000.

[7] TICRA Engineering Consultants, "SNIFTD: Software package for Spherical Near-Field Far-Field Transformations with Full Probe Correction," Kron Prinsens Gade 13, DK-1114 Copenhagen K, Denmark.

[8] C. A. Balanis, *Advanced Engineering Electromagnetics*. New York: Wiley, 1989.

**Fernando Las-Heras** was born in Zaragoza, Spain, in 1963. He received the M.S. and Ph.D. degrees, both in telecommunication engineering, from the Universidad Politécnica de Madrid (UPM), Madrid, Spain, in 1987 and 1990, respectively.

From 1988 to 1990, he was a National Graduate Research Fellow. From 1991 to 2000, he held the position of Associate Professor in the Department of Signals, Systems and Radiocommunications, UPM. He has participated in a great number of research and development projects and is the author of communications and papers regarding research topics in numerical methods applied to electromagnetics, high-frequency methods for RCS estimation, analysis, and design of antennas, and electromagnetic inverse problems with application to antenna measurement and synthesis. He is presently in charge of the area of Signal, Theory and Communication, University of Oviedo, Oviedo, Spain.

**Tapan K. Sarker** (S'69–M'76–SM'81–F'92) received the B.Tech. degree from the Indian Institute of Technology, Kharagpur, India, in 1969, the M.Sc.E. degree from the University of New Brunswick, Frederiton, NB, Canada, in 1971, and the M.S. and Ph.D. degrees from Syracuse University, Syracuse, NY, in 1975.

From 1975 to 1976, he was with the TACO Division, General Instruments Corporation. He was with Rochester Institute of Technology, Rochester, NY, from 1976 to 1985. He was a Research Fellow with the Gordon McKay Laboratory, Harvard University, Cambridge, MA, from 1977 to 1978. He is now a Professor with the Department of Electrical and Computer Engineering, Syracuse University, Syracuse, NY. His current research interests deal with numerical solutions of operator equations arising in electromagnetics and signal processing with application to system design. He has authored or coauthored more than 210 journal articles and numerous conference papers, he has written chapters in 28 books and has published ten books including *Iterative and Self Adaptive Finite-Elements in Electromagnetic Modeling* (Artech House: Norwood, MA, 1998).

Dr. Sarkar is a Registered Professional Engineer in the State of New York. He received one of the "best solution" awards in May 1977 at the Rome Air Development Center (RADC) Spectral Estimation Workshop. He received the Best Paper Award at the IEEE Transactions on Electromagnetic Compatibility Conference in 1979 and in the 1997 National Radar Conference. He received the College of Engineering Research Award in 1996 and the Chancellor's Citation for Excellence in Research in 1998 from Syracuse University. He was an Associate Editor for feature articles of the IEEE ANTENNAS AND PROPAGATION SOCIETY NEWSLETTER, and he was the Technical Program Chairman for the 1988 IEEE Antennas and Propagation Society International Symposium and URSI Radio Science Meeting. From 1995 to 2000, he was the Chapter Chair for the local AP/MTT section. He is on the editorial board of the *Journal of Electromagnetic Waves and Applications* and *Microwave and Optical Technology Letters*. He has been appointed U.S. Research Council Representative to many URSI General Assemblies. He was the Chairman of the Intercommission Working Group of International URSI on Time Domain Metrology (1990-1996). He is a member of Sigma Xi and International Union Radio Science Commissions A and B. He received the title of Docteur Honoris Causa from the Universite Blaise Pascal, Clermont Ferrand, France, in 1998, and the medal of the City Clermont Ferrand, France, in 2000.